J|A|C|S
ARTICLES
Published on Web 10/18/2006

Persistent Electron-Transfer State of a π-Complex of Acridinium Ion Inserted between Porphyrin Rings of Cofacial Bisporphyrins

Makiko Tanaka,[†] Kei Ohkubo,[†] Claude P. Gros,[‡] Roger Guilard,*[,‡] and Shunichi Fukuzumi*[,†]

Contribution from the Department of Material and Life Science, Graduate School of Engineering, Osaka University, SORST, Japan Science and Technology Agency, Suita, Osaka 565-0871, Japan, and LIMSAG, UMR 5633, Université de Bourgogne, 9, Avenue Alain Savary, BP 47870, 21078 Dijon Cedex, France

Received July 1, 2006; E-mail: Roger.Guilard@u-bourgogne.fr; fukuzumi@chem.eng.osaka-u.ac.jp

Abstract: A free-base cofacial bisporphyrin, H_4DPOx, forms a π-complex with acridinium ion (AcH^+) by $\pi-\pi$ interaction in benzonitrile (PhCN). Formation of the H_4DPOx$-AcH^+$ π-complex was probed by UV−vis and NMR spectroscopy. The binding constant between AcH^+ and H_4DPOx is determined as 9.7×10^4 M^{-1}. Photoinduced electron transfer (ET) from the H_4DPOx to the AcH^+ moiety occurred efficiently in the π-complex to form the ET state ($H_4DPOx^{\bullet+}-AcH^{\bullet}$). The ET state is successfully detected by laser flash photolysis. The lifetime of the ET state is 18 μs in PhCN at 298 K, and the quantum yield of the ET state is 90%. The temperature dependence of the ET state lifetime has been examined in the range from 273 to 353 K. The ET state lifetime exhibited a large temperature dependence, and the linear plot of $\ln(k_{BET}T^{1/2})$ vs T^{-1}, in accordance with the Marcus equation, affords the ET reorganization energy (0.54 eV). As a result, a remarkably long-lived ET state has been attained at low temperature, and virtually no decay of the ET state was observed at 77 K. Such an extremely long-lived ET state is indeed detected by steady-state UV−vis absorption spectroscopy.

Introduction

The natural photosynthetic system consists of light-harvesting antenna units and reaction center units. In the photosynthetic reaction centers of purple bacteria, there are four bacteriochlorophylls, two bacteriopheophytins, two ubiquinones (Q_A and Q_B), and a non-heme iron atom. Light-initiated charge separation occurs between the special pair and the neighboring pigments, finally leading to a special pair radical cation and radical anion $Q_B^{\bullet-}$. The electron-transfer process is found to occur very rapidly, with nearly 100% quantum yield.[1−3] The charge-separated state efficiently converts into chemical energy, because this lifetime is quite long (∼1 s). Each component of the photosynthetic reaction center is located at the right position by noncovalent bonding in the protein matrix to optimize the charge-separation efficiency.[4] The use of noncovalent bonding, such as metal−ligand coordination, electrostatic interaction, hydrogen bonds, and rotaxane formation, has recently merited increasing attention as a simpler but more elegant way to construct electron donor−acceptor ensembles mimicking the efficient biological electron-transfer systems.[5−21] In particular, $\pi-\pi$ interaction has merited increasing attention as one of the

[†] Osaka University.
[‡] Université de Bourgogne.

(1) *Anoxygenic Photosynthetic Bacteria*; Blankenship, R. E., Madigan, M. T., Bauer, C. E., Eds.; Kluwer Academic Publisher: Dordecht, 1995.
(2) *The Photosynthetic Reaction Center*; Deisenhofer, J., Norris, J. R., Eds.; Academic Press: San Diego, 1993.
(3) McDermott, G.; Prince, S. M.; Freer, A. A.; Hawthornthwaite-Lawless, A. M.; Papiz, M. Z.; Cogdell, R. J.; Isaacs, N. W. *Nature* **1995**, *374*, 517.
(4) (a) Diesenhofer, J.; Michel, H. *Angew. Chem., Int. Ed. Engl.* **1989**, *28*, 829. (b) Feher, G.; Allen, J. P.; Okamura, M. Y.; Rees, D. C. *Nature* **1989**, *339*, 111.
(5) (a) Lehn, J.-M. *Supramolecular Chemistry: Concepts and Perspectives*; VCH: Weinheim, 1995. (b) Sessler, J. L.; Wang, B.; Springs, S. L.; Brown, C. T. In *Comprehensive Supramolecular Chemistry*; Atwood, J. L., Davies, J. E. D., Eds.; Pergamon: New York, 1996.
(6) Chang, C. J.; Brown, J. D. K.; Chang, M. C. Y.; Baker, E. A.; Nocera, D. G. In *Electron Transfer in Chemistry*; Balzani, V. Ed.; Wiley-VCH: Weinheim, 2001; Vol. 3, pp 409−461.
(7) (a) Hunter, C. A.; Sanders, J. K. M.; Beddard, G. S.; Evans, S. *J. Chem. Soc., Chem. Commun.* **1989**, 1765. (b) Anderson, H. L.; Hunter, C. A.; Sanders, J. K. M. *J. Chem. Soc., Chem. Commun*. **1989**, 226.
(8) (a) de Rege, P. J. F.; Williams, S. A.; Therien, M. J. *Science* **1995**, *269*, 1409. (b) Harriman, A.; Magda, D. J.; Sessler, J. L. *J. Chem. Soc., Chem. Commun.* **1991**, 345. (c) Sessler, J. L.; Wang, B.; Harriman, A. *J. Am. Chem. Soc.* **1995**, *117*, 704. (d) Berman, A.; Izraeli, E. S.; Levanon, H.; Wang, B.; Sessler, J. L. *J. Am. Chem. Soc.* **1995**, *117*, 8252.
(9) (a) Hayashi, T.; Ogoshi, H. *Chem. Soc. Rev.* **1997**, *26*, 355. (b) Blanco, M.-J.; Jiménez, M. C.; Chambron, J.-C.; Heitz, V.; Linke, M.; Sauvage, J.-P. *Chem. Soc. Rev.* **1999**, *28*, 293. (c) Willner, I.; Kaganer, E.; Joselevich, E.; Dürr, H.; David, E.; Günter, M. J.; Johnston, M. R. *Coord. Chem. Rev.* **1998**, *171*, 261.
(10) (a) D'Souza, F.; Rath, N. P.; Deviprasad, G. R.; Zandler, M. E. *Chem. Commun*. **2001**, 267. (b) D'Souza, F.; Deviprasad, G. R.; El-Khouly, M. E.; Fujitsuka, M.; Ito, O. *J. Am. Chem. Soc.* **2001**, *123*, 5277. (c) D'Souza, F.; Deviprasad, G. R.; Rahman, M. S.; Choi, J. *Inorg. Chem*. **1999**, *38*, 2157. (d) D'Souza, F.; Zandler, M. E.; Smith, P. M.; Deviprasad, G. R.; Arkady, K.; Fujitsuka, M.; Ito, O. *J. Phys. Chem. A* **2002**, *106*, 649.
(11) (a) Da Ros, T.; Prato, M.; Guldi, D. M.; Ruzzi, M.; Pasimeni, L. *Chem. Eur. J*. **2001**, *7*, 816. (b) D'Souza, F. *J. Am. Chem. Soc*. **1996**, *118*, 923. (c) El-Khouly, M. E.; Rogers, L. M.; Zandler, M. E.; Suresh, G.; Fujitsuka, M.; Ito, O.; D'Souza, F. *ChemPhysChem* **2003**, *4*, 474. (d) D'Souza, F.; Deviprasad, G. R.; Zandler, M. E.; El-Khouly, M. E.; Fujitsuka, M.; Ito, O. *J. Phys. Chem. B* **2002**, *106*, 4952.
(12) (a) Otsuki, J.; Harada, K.; Toyama, K.; Hirose, Y.; Araki, K.; Seno, M.; Takatera, K.; Watanabe, T. *Chem. Commun*. **1998**, 1515. (b) Imahori, H.; Yoshizawa, E.; Yamada, K.; Hagiwara, K.; Okada, T.; Sakata, Y. *J. Chem. Soc., Chem. Commun.* **1995**, 1133.

10.1021/ja064678b CCC: $33.50

Scheme 1

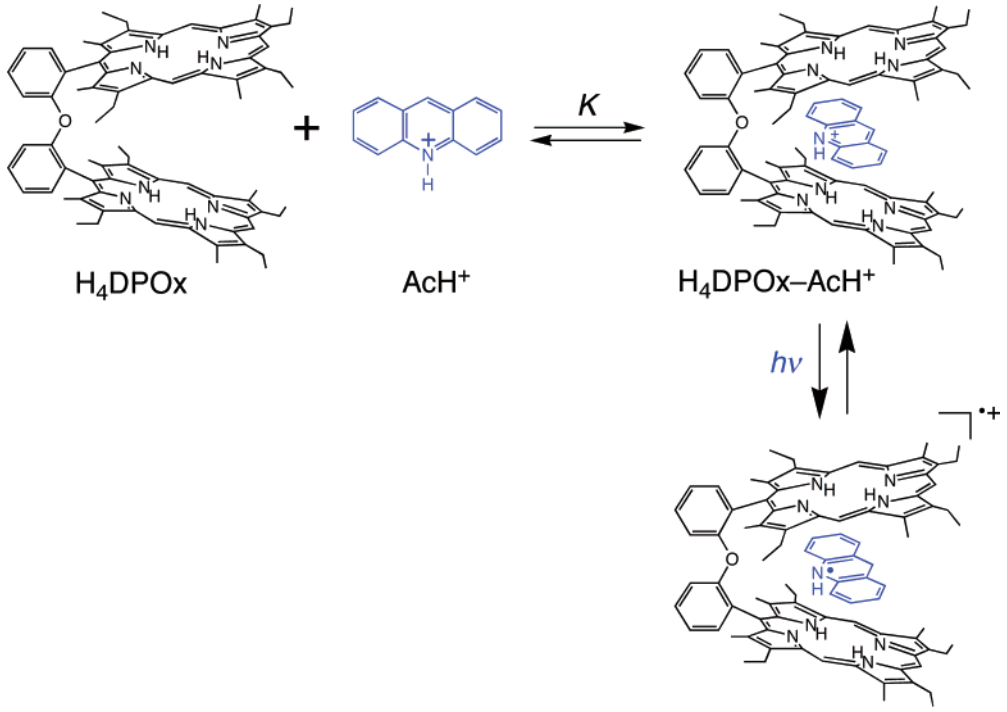

most important types of noncovalent binding because of its important role in biological systems, such as for π-stacking of double-strand DNA.[22] For example, a bisporphyrin has been shown to form a π-complex with fullerene, which is inserted between the two porphyrin rings.[23] A DNA intercalator such as acridinium ion can also be inserted between the two porphyrin rings of a water-soluble bisporphyrin to form a π-complex.[24] Acridinium ion is suitable as a component of an artificial photosynthetic reaction center because of the small reorganization energy (λ) of electron transfer,[25] which results in fast photoinduced electron transfer but extremely slow back electron transfer.[26] However, there has been no report on the photodynamics of π-complexes of acridinium ion with electron donors.

We report herein the formation of a π-complex of a free-base bisporphyrin (H_4DPOx) with acridinium perchlorate ($AcH^+ClO_4^-$) and the photodynamics in benzonitrile (PhCN), as shown in Scheme 1. H_4DPOx is regarded as a model compound of [$(BChl)_2$], which has two cofacial porphyrin rings and a flexible spacer, diphenyl oxide. The formation of the electron-transfer (ET) state is examined by laser flash photolysis experiments. The decay of the ET state has been found to be highly temperature dependent. As a result, a remarkably long-lived ET state has been attained at low temperature, and virtually no decay of the ET state was observed at 77 K (vide infra).

Experimental Section

Materials. The synthesis details and analytical data for H_4DPOx are shown in the Supporting Information, S1−S3. Similar systems have been reported in the literature.[27] 5,10,15,20-Tetraphenyl-21*H*,23*H*-porphyrin (H_2TPP) and 2,3,7,8,12,13,17,18-octaethyl-21*H*,23*H*-porphyrin (H_2OEP) were obtained from Aldrich Chemical Co. Perchloric

(13) (a) Martínez-Díaz, M. V.; Fender, N. S.; Rodríguez-Morgade, M. S.; Gómez-López, M.; Diederich, F.; Echegoyen, L.; Stoddart, J. F.; Torres, T. *J. Mater. Chem.* **2002**, *12*, 2095. (b) Guldi, D. M.; Ramey, J.; Martínez-Díaz, M. V.; de la Escosura, A.; Torres, T.; Da Ros, T.; Prato, M. *Chem. Commun.* **2002**, 2774. (c) Guldi, D. M.; Gouloumis, A.; Vázquez, P.; Torres, T.; Georgakilas, V.; Prato, M. *J. Am. Chem. Soc.* **2005**, *127*, 5811. (d) de la Escosura, A.; Martínez-Díaz, M. V.; Thordarson, P.; Rowan, A. E.; Nolte, R. J. M.; Torres, T. *J. Am. Chem. Soc.* **2003**, *125*, 12300. (e) de la Escosura, A.; Martínez-Díaz, M. V.; Guldi, D. M.; Torres, T. *J. Am. Chem. Soc.* **2006**, *128*, 4112. (f) Ballesteros, B.; de la Torre, G.; Torres, T.; Hug, G. L.; Rahman, G. M. A.; Guldi, D. M. *Tetrahedron* **2006**, *62*, 2097.
(14) (a) D'Souza, F.; Deviprasad, G. R.; Zandler, M. E.; El-Khouly, M. E.; Fujitsuka, M.; Ito, O. *J. Phys. Chem. A* **2003**, *107*, 4801. (b) El-Khouly, M. E.; Gadde, S.; Deviprasad, G. R.; Fujitsuka, M.; Ito, O.; D'Souza, F. *J. Porphyrins Phthalocyanines* **2003**, *7*, 1. (c) D'Souza, F.; Deviprasad, G. R.; Zandler, M. E.; Hoang, V. T.; Klykov, A.; Van Stipdonk, M.; Perera, A.; El-Khouly, M. E.; Fujitsuka, M.; Ito, O. *J. Phys. Chem. A* **2002**, *106*, 3243.
(15) Flamigni, L.; Talarico, A. M.; Serroni, S.; Puntoriero, F.; Gunter, M. J.; Johnston, M. R.; Jeynes, T. P. *Chem. Eur. J.* **2003**, *9*, 2649. (b) Benniston, A. C.; Davies, M.; Harriman, A.; Sams, C. *J. Phys. Chem. A* **2003**, *107*, 4669.
(16) Nelissen, H. F. M.; Kercher, M.; De Cola, L.; Feiters, M. C.; Nolte, R. J. M. *Chem. Eur. J.* **2002**, *8*, 5407.
(17) (a) Lainé, P.; Bedioui, F.; Amouyal, E.; Albin, V.; Berruyer-Penaud, F. *Chem. Eur. J.* **2002**, *8*, 3162. (b) Lainé, P.; Bedioui, F.; Ochsenbein, P.; Marvaud, V.; Bonin, M.; Amouyal, E. *J. Am. Chem. Soc.* **2002**, *124*, 1364.
(18) Kashiwagi, Y.; Imahori, H.; Araki, Y.; Ito, O.; Yamada, K.; Sakata, Y.; Fukuzumi, S. *J. Phys. Chem. A* **2003**, *107*, 5515.
(19) Okamoto, K.; Fukuzumi, S. *J. Phys. Chem. B* **2005**, *109*, 7713.
(20) Hasobe, T.; Imahori, H.; Kamat, P. V.; Ahn, T. K.; Kim, S. K.; Kim, D.; Fujimoto, A.; Hirakawa, T.; Fukuzumi, S. *J. Am. Chem. Soc.* **2005**, *127*, 1216.
(21) (a) Hunter, C. A.; Sanders, J. K. M. *J. Am. Chem. Soc.* **1990**, *112*, 5525. (b) Leighton, P.; Cowan, J. A.; Abraham, R. J.; Sanders, J. K. M. *J. Org. Chem.* **1988**, *53*, 733.
(22) (a) Lewis, F. D.; Liu, X.; Liu, J.; Miller, S. E.; Hayes, R. T.; Wasielewski, M. R. *Nature* **2000**, *406*, 51. (b) Barnett, R. N.; Cleveland, C. L.; Joy, A.; Landman, U.; Schuster, G. B. *Science* **2001**, *294*, 567. (c) Treadway, C. R.; Hill, M. G.; Barton, J. K. *Chem. Phys.* **2002**, *281*, 409. (d) Giese, B.; Amaudrut, J.; Kohler, A.-K.; Spormann, M.; Wessely, S. *Nature* **2001**, *412*, 318. (e) Tashiro, R.; Sugiyama, H. *J. Am. Chem. Soc.* **2003**, *125*, 15282.
(23) (a) Sun, D.; Tham, F. S.; Reed, C. A.; Chaker, L.; Burgess, M.; Boyd, P. D. W. *J. Am. Chem. Soc.* **2000**, *122*, 10704. (b) Sun, D.; Tham, F. S.; Reed, C. A.; Chaker, L.; Boyd, P. D. W. *J. Am. Chem. Soc.* **2002**, *124*, 6604.
(24) (a) Mizutani, T.; Wada, K.; Kitagawa, S. *J. Am. Chem. Soc.* **2001**, *123*, 6459. (b) Wada, K.; Mizutani, T.; Matsuoka, H.; Kitagawa, S. *Chem. Eur. J.* **2003**, *9*, 2368.
(25) (a) Fukuzumi, S.; Ohkubo, K.; Suenobu, T.; Kato, K.; Fujitsuka, M.; Ito, O. *J. Am. Chem. Soc.* **2001**, *123*, 8459. (b) Fukuzumi, S.; Nishimine, M.; Ohkubo, K.; Tkachenko, N. V.; Lemmetyinen, H. *J. Phys. Chem. B* **2003**, *107*, 12511.
(26) (a) Fukuzumi, S.; Kotani, H.; Ohkubo, K.; Ogo, S.; Tkachenko, N. V.; Lemmetyinen, H. *J. Am. Chem.* Soc. **2004**, *126*, 1600. (b) Kotani, H.; Ohkubo, K.; Fukuzumi, S. *J. Am. Chem. Soc.* **2004**, *126*, 15999. (c) Ohkubo, K.; Kotani, H.; Fukuzumi, S. *Chem. Commun.* **2005**, 4520.
(27) (a) Faure, S.; Stern, C.; Guilard, R.; Harvey, P. D. *J. Am. Chem. Soc.* **2004**, *126*, 1253. (b) Bolze, F.; Gros, C. P.; Drouin, M.; Espinosa, E.; Harvey P. D.; Guilard, R. *J. Organomet. Chem.* **2002**, *89*, 643.

acid was obtained from Wako Pure Chemical Industries, Ltd. Acridine was obtained from Tokyo Kasei Organic Chemicals. Tetra-*n*-butylammonium hexafluorophosphate ($TBAPF_6$), used as a supporting electrolyte for electrochemical measurements, was purchased from Tokyo Kasei Organic Chemicals, recrystallized from EtOH/water, and dried in vacuo according to the standard procedure.[28] PhCN and butyronitrile were distilled with P_2O_5 in vacuo.[29] Chloroform ($CHCl_3$) and 2-methyltetrahydrofuran (2-MeTHF) were used as received. Tris(2,2′-bipyridyl)ruthenium(II) chloride hexahydrate $[Ru(bpy)_3Cl_2 \cdot 6H_2O]$ was obtained from Aldrich. Tris(2,2′-bipyridyl)ruthenium(III) hexafluorophosfate $[Ru(bpy)_3(PF_6)_3]$ was prepared by oxidizing $Ru(bpy)_3^{2+}$ with lead dioxide in aqueous H_2SO_4, followed by the addition of KPF_6.[30] Ferrocene (Wako Pure Chemicals) was obtained commercially and purified by sublimation.

Synthesis of $AcH^+ClO_4^-$. Acridinium perchlorate ($AcH^+ClO_4^-$) was prepared by the reaction of acridine with perchloric acid in acetone at room temperature for 3 h. $AcH^+ClO_4^-$ was rinsed with cold water and recrystallized from MeOH−H_2O (85:15). ^{1}H NMR (300 MHz, $CDCl_3$): δ 14.98 (brs, 1H), 9.44 (s, 1H), 8.63 (d, J = 9.0 Hz, 2H), 8.24 (d, J = 8.4 Hz, 2H), 8.17 (t, J = 7.8 Hz, 2H), 7.83 (t, J = 7.7 Hz, 2H). MALDI-TOF MS: m/z 180 (M). Anal. Calcd for $C_{13}H_{10}ClNO_4$: C, 55.83; H, 3.60; N, 5.01. Found: C, 55.70; H, 3.47; N, 5.03.

^{1}H NMR spectra were measured on a JEOL JMN-AL300 (300 MHz) instrument. Matrix-assisted laser desorption/ionization (MALDI) time-of-flight (TOF) mass spectra were measured on a Kratos Compact MALDI I (Shimadzu).

Caution! *The organic perchlorate salt may be exploded. All measurements should be manipulated with care.*

Spectral Measurements. UV−visible spectra were recorded on a Shimadzu UV-3100PC spectrometer or a Hewlett-Packard 8453 diode array spectrophotometer at 298 K. The formation of the electron-transfer state $H_4DPOx^{\bullet+}$−$AcH^{\bullet}$ was examined by studying the change in the UV−visible spectrum of a deaerated 2-MeTHF solution containing a 10% butyronitrile solution of H_4DPOx (1.8×10^{-5} M) and AcH^+ (3.6×10^{-4} M) at 77 K after photoirradiation at low temperature with a high-pressure mercury lamp (USH-1005D) through a water filter using a Hewlett-Packard 8453 diode array spectrophotometer. The UV−visible spectra were taken with a quartz tube (3 mm i.d.) in liquid N_2 dewar.

Laser Flash Photolysis Measurements. For the nanosecond laser flash photolysis experiments, deaerated PhCN solutions were excited by a Panther OPO pumped by a Nd:YAG laser (Continuum, SLII-10, 4−6 ns fwhm) at λ = 430 nm, 520 nm. The photodynamics was monitored by continuous exposure to a xenon lamp (150 W) as a probe light and a photomultiplier tube (Hamamatsu 2949) as a detector. The transient spectra were recorded using fresh solutions in each laser excitation. The solution was deoxygenated by argon purging for 15 min prior to measurements. The experiments at various temperatures were performed using a Unisoku thermostated cell holder.

Fluorescence Lifetime Measurements. Fluorescence decays were measured by using a Photon Technology International GL-3300 nitrogen laser with a Photon Technology International GL-302 dye laser and a nitrogen laser/pumped dye laser system equipped with a four-channel digital delay/pulse generator (Standard Research System Inc., model DG535) and a motor driver (Photon Technology International, model MD-5020). The excitation wavelength was 525 nm with use of coumarin 540A (Exciton Co., Ltd.).

Phosphorescence Measurements. H_4DPOx in 50% EPA (5:5:2 2-propanol/diethyl ether/ethanol) and 50% ethyl iodide at 77 K was excited at λ = 575 nm using a Cosmo System LVU-200S spectrometer. A photomultiplier (Hamamatsu Photonics model R5509-72) was used to detect emission in the near-infrared region (band path 2 mm).

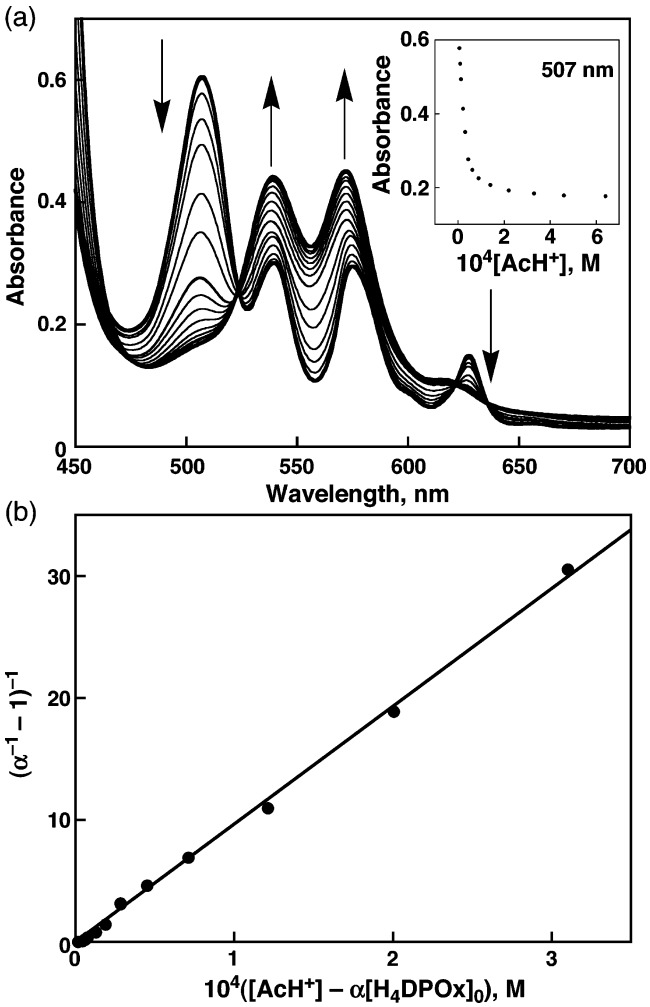

Figure 1. (a) UV−visible spectra of H_4DPOx (2.0×10^{-5} M) in the presence of various concentrations of AcH^+ (0−9.3×10^{-4} M) in PhCN. The arrows indicate the direction of change. Inset: Plot of the absorbance vs $[AcH^+]$ at 507 nm. (b) Plot of $(\alpha^{-1} - 1)^{-1}$ vs $([AcH^+] - \alpha[H_4DPOx]_0)$ at 507 nm for the π-complex formation of H_4DPOx with AcH^+.

Electrochemical Measurements. Measurements of the cyclic voltammetry (CV), the differential pulse voltammetry (DPV), and the second harmonic AC voltammetry (SHACV)[31] were performed at 298 K, using a BAS 100W electrochemical analyzer in a deaerated solvent containing 0.10 M $TBAPF_6$ as a supporting electrolyte at 298 K. A conventional three-electrode cell was used with a platinum working electrode and a platinum wire as a counter electrode. The measured potentials were recorded with respect to the $Ag/AgNO_3$ (1.0×10^{-2} M). The E_{ox} and E_{red} values (vs $Ag/AgNO_3$) are converted to those vs SCE by adding 0.29 V, respectively.[32] All electrochemical measurements were carried out under an atmospheric pressure of argon.

Electron Spin Resonance (ESR) Measurements. An argon-saturated PhCN solution of H_4DPOx (3.5×10^{-6} M) and AcH^+ (1.7×10^{-5} M) was irradiated at 173 K with a high-pressure mercury lamp (USH-1005D) through a water filter focused at the sample cell in the ESR cavity. The ESR spectra were taken on a JEOL JES-RE1XE spectrometer and were recorded under nonsaturating microwave power conditions. The magnitude of the modulation was chosen to optimize

(28) Bedard, R. L.; Dahl, L. F. *J. Am. Chem. Soc.* **1986**, *108*, 5933.
(29) Perrin, D. D.; Armarego, W. L. F.; Perrin, D. R. *Purification of Laboratory Chemicals*, 4th ed.; Pergamon Press: Elmsford, NY, 1996.
(30) DeSimone, R. E.; Drago, R. S. *J. Am. Chem. Soc.* **1970**, *92*, 2343.
(31) The SHACV method provides a superior approach to directly evaluating the one-electron redox potentials in the presence of a follow-up chemical reaction, relative to the better-known dc and fundamental harmonic ac methods: (a) Bond, A. M.; Smith, D. E. *Anal. Chem.* **1974**, *46*, 1946. (b) Arnett, E. M.; Amarnath, K.; Harvey, N. G.; Cheng, J. *J. Am. Chem. Soc.* **1990**, *112*, 344.
(32) Mann, C. K.; Barnes, K. K. *Electrochemical Reactions in Non-aqueous Systems*; Marcel Dekker: New York, 1970.

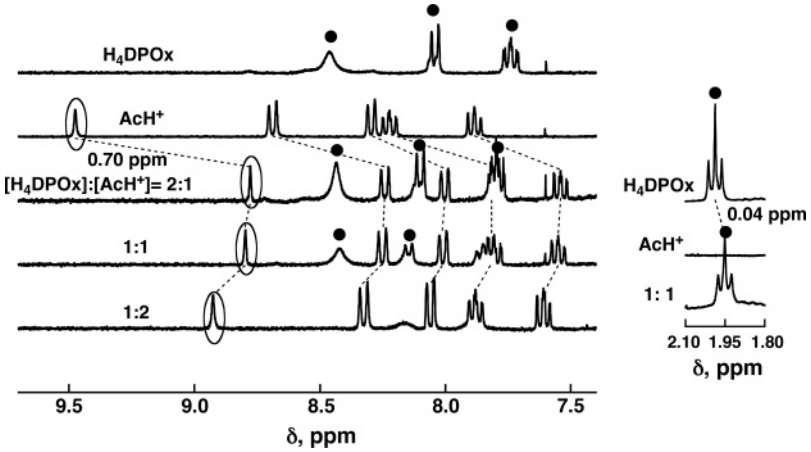

Figure 2. ^{1}H NMR spectra of H_4DPOx, AcH^+, [H_4DPOx]:[AcH^+] = 2:1, [H_4DPOx]:[AcH^+] = 1:1, and [H_4DPOx]:[AcH^+] = 1:2 in $CDCl_3$. Closed circles denote the signals due to H_4DPOx.

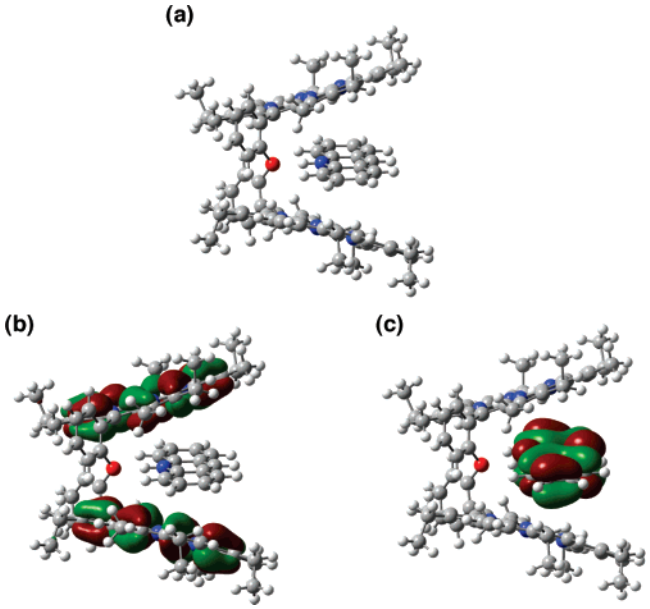

Figure 3. (a) Structure of H_4DPOx−AcH^+ optimized by DFT calculation. (b) HOMO and (c) LUMO orbitals calculated by a DFT method at the B3LYP/6-31G*//B3LYP/3-21G level.

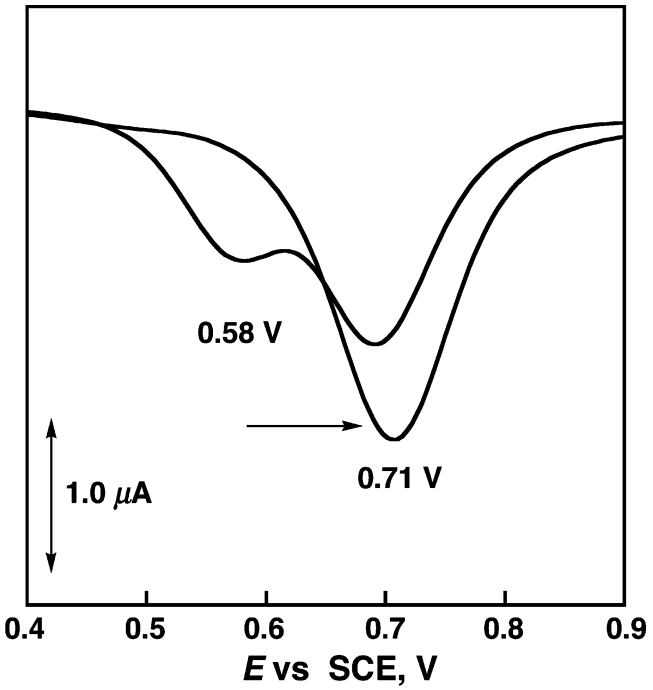

Figure 4. DPV of H_4DPOx (3.2×10^{-4} M) in the absence and in the presence of AcH^+ (4.6×10^{-4} M) in deaerated PhCN containing $TBAPF_6$ (0.10 M) at 298 K. The arrows indicate the direction of change. Sweep rate: 10 mV s^{-1}.

the resolution and the signal-to-noise ratio (S/N) of the observed spectra. The *g* values were calibrated using an Mn^{2+} marker.

Theoretical Calculations. Density-functional theory (DFT) calculations were performed on an 8 CPU workstation (PQS, Quantum Cube QS8-2400C-064). Geometry optimizations were carried out using the Becke3LYP functional and 6-31G* basis set,[33,34] with the restricted Hartree−Fock (RHF) formalism and as implemented in the Gaussian 03 program, revision C.02.[35] Graphical outputs of the computational results were generated with the Gauss View software program (version 3.09) developed by Semichem, Inc.[36]

Results and Discussion

***π*-Complex Formation between H_4DPOx and AcH^+.** Formation of the H_4DPOx−AcH^+ complex was probed by UV−visible and NMR spectroscopy; the spectra are shown in Figures 1 and 2, respectively. The UV−vis spectra of H_4DPOx in PhCN at 298 K are changed upon addition of AcH^+, where the number of Q-bands changes from four to two with isosbestic points due to the complex formation between H_4DPOx and AcH^+ (Figure 1a). The Job's plot obtained by the UV−vis spectral titration indicates that H_4DPOx forms a 1:1 complex with AcH^+ (see Supporting Information, S5).[37] In such a case, the absorbance change is given by eq 1,[38]

$$(\alpha^{-1} - 1)^{-1} = K([AcH^+] - \alpha[H_4DPOx]_0) \qquad (1)$$

(33) (a) Becke, A. D. *J. Chem. Phys.* **1993**, *98*, 5648. (b) Lee, C.; Yang, W.; Parr, R. G. *Phys. Rev. B* **1988**, *37*, 785.
(34) Hehre, W. J.; Radom, L.; Schleyer, P. v. R.; Pople, J. A. *Ab Initio Molecular Orbital Theory*; Wiley: New York, 1986.
(35) Frisch, M. J.; et al. *Gaussian 03*, Revision C.02; Gaussian, Inc.: Wallingford, CT, 2004.
(36) Dennington, R., II; Keith, T.; Millam, J.; Eppinnett, K.; Hovell, W. L.; Gilliland, R. *Gauss View*, Version 3.09; Semichem, Inc.: Shawnee Mission, KS, 2003.
(37) The Job's plot in S5 indicates a small contribution of a 1:2 complex formed between H_4DPOx and AcH^+. Formation of a 1:1 complex as a major species is well verified from the linear plot of eq 1 (see Figure 1b).
(38) Fukuzumi, S.; Kondo, Y.; Mochizuki, S.; Tanaka, T. *J. Chem. Soc., Perkin Trans. 2* **1989**, 1753.

Table 1. Redox Potentials of H_4DPOx, AcH^+, and H_4DPOx−AcH^+ and Energy Level of ET State ($-\Delta G_{ET}$) in Deaerated PhCN

compound	E_{ox} vs SCE, V, for H_4DPOx	E_{ox} vs SCE, V, for AcH^+	$-\Delta G_{ET}$, eV
H_4DPOx	0.58		
AcH^+		−0.46	
H_4DPOx−AcH^+	0.71	−0.57	1.28

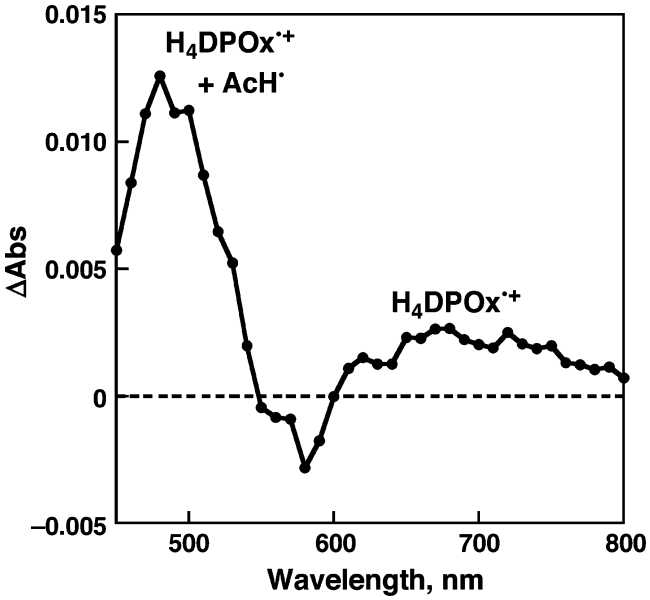

Figure 5. Transient absorption spectrum of H_4DPOx (3.4×10^{-5} M) in the presence of AcH^+ (3.3×10^{-4} M) in deaerated PhCN at 273 K, taken 20 μs after laser excitation at 520 nm.

where $\alpha = (A - A_0)/(A_\infty - A_0)$; A_0 and A are the absorbance of H_4DPOx at 507 nm in the absence and presence of AcH^+, respectively. From a linear correlation between $(\alpha^{-1} - 1)^{-1}$ and $([AcH^+] - \alpha[H_4DPOx]_0)$, the formation constant (K) of the H_4DPOx−AcH^+ complex is determined as 97 000 ± 1000 M^{-1} in PhCN (see Figure 1b).

The π-complex formation is also confirmed by ^{1}H NMR. The ^{1}H NMR signals of both H_4DPOx and AcH^+ exhibit upfield shifts upon complexation in $CDCl_3$, as shown in Figure 2. The signals of both H_4DPOx and AcH^+ are shifted depending on the mixture ratio, and the largest upfield shift is observed with a 1:1 concentration ratio of AcH^+ and H_4DPOx. Especially the signals of AcH^+ show larger shifts upon complexation owing to the influence of the porphyrin ring current effect. The C9 proton of AcH^+ is shifted by 0.70 ppm upon the insertion of AcH^+ between two porphyrin rings. The change in the chemical shift in the case of monomer porphyrin (H_2OEP, OEP = octaethylporphyrin) is smaller than that of the shift observed in the case of the bisporphyrin (H_4DPOx) (see Supporting Information, S6). These results suggest that AcH^+ is inserted between the two porphyrin rings of the bisporphyrin. In the presence of excess AcH^+, the shift of AcH^+ becomes smaller due to the fast exchange of AcH^+ inserted between two porphyrin rings with that of the free ion in solution on the NMR time scale.

The geometry optimization of the π-complex between H_4DPOx and AcH^+ was performed by DFT calculation at the B3LYP/3-21G basis set (see Experimental Section). The structure of the π-complex between H_4DPOx and AcH^+, optimized by DFT calculation, is shown in Figure 3a. The HOMO (highest occupied molecular orbital) and LUMO (lowest unoccupied molecular orbital) of $H_4DPOx^{\bullet+}$−$AcH^{\bullet}$ are localized on the porphyrin and AcH^+ moieties, as shown in Figure 3b and c, respectively.

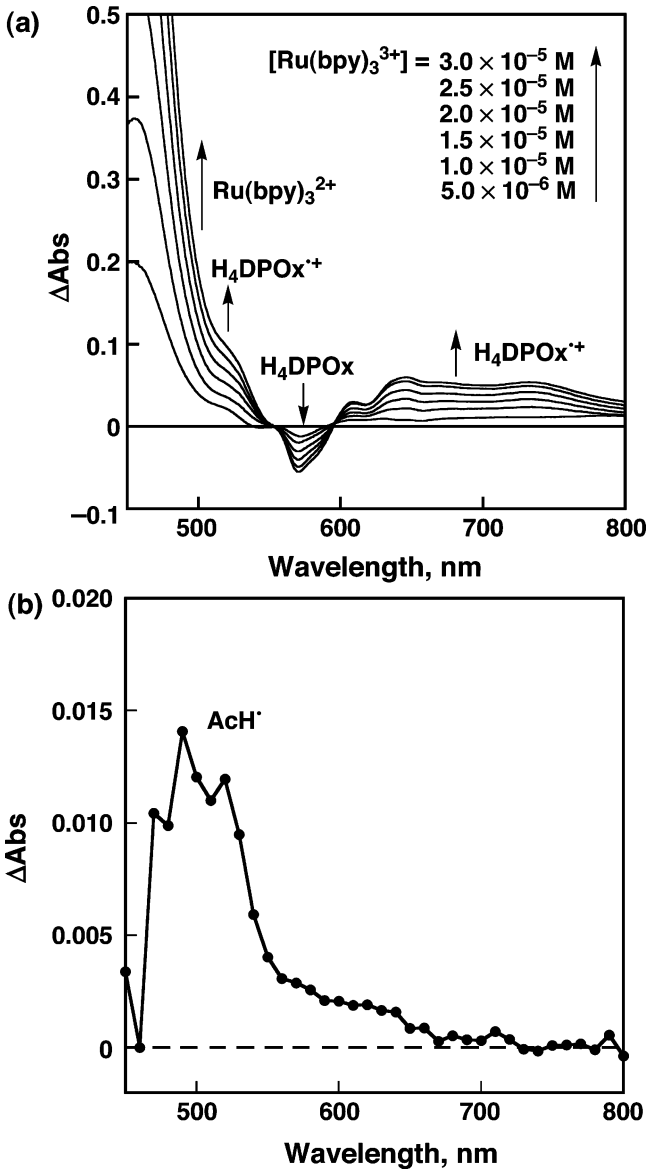

Figure 6. (a) Difference absorption spectra in the ET oxidation of the H_4DPOx−AcH^+ complex ($[H_4DPOx] = 3.0 \times 10^{-5}$ M, $[AcH^+] = 3.3 \times 10^{-4}$ M) with various concentrations of $Ru(bpy)_3^{3+}$ (1.0×10^{-5}−3.0×10^{-5} M) in deaerated PhCN. The strong AcH^+ complex, with an absorption band of H_4DPOx, is overlapped with that of $Ru(bpy)_3^{2+}$ around 450−520 nm. (b) Transient absorption spectrum of AcH^+ (1.6×10^{-4} M) in the presence of ferrocene (2.7×10^{-3} M) in deaerated PhCN at 298 K, taken 2 μs after laser excitation at 430 nm.

The change in the one-electron oxidation potential of the bisporphyrin upon complex formation with AcH^+ was examined by differential pulse voltammetry (DPV) as shown in Figure 4. The one-electron oxidation potential of H_4DPOx (E_{ox}) is changed from 0.58 V in the absence of AcH^+ to 0.71 V after the insertion of AcH^+. In the π-complex, the bisporphyrin becomes more difficult to be oxidized because of the repulsion of plus charges between the porphyrin radical cation and AcH^+ when the first and second one-electron oxidations virtually coincide (Figure 4).

The one-electron reduction potential of AcH^+ was also changed, from −0.46 V in the absence of the bisporphyrin to

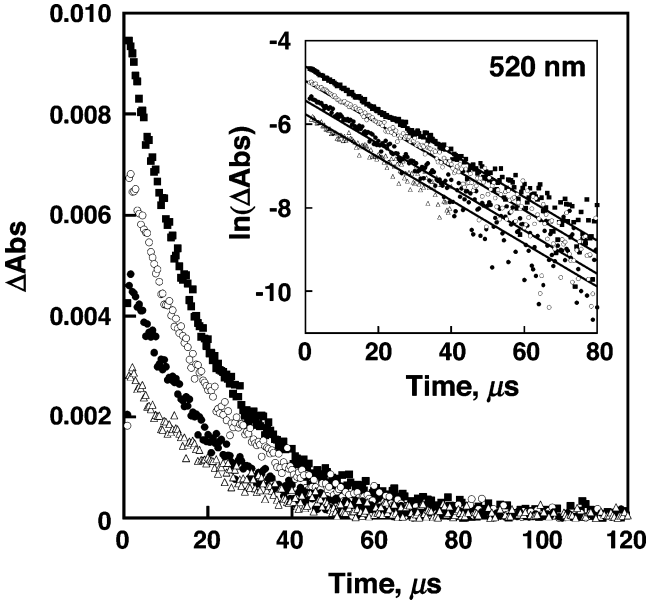

Figure 7. Time profiles of the absorption at 520 nm of $H_4DPOx^{\bullet+}-AcH^{\bullet}$ obtained with different laser intensities [1.5 (△), 1.9 (●), 2.1 (○), and 3.8 (■) mJ/pulse] in deaerated PhCN at 298 K. (b) Time profiles of the absorption at 460 nm of $H_4DPOx^{\bullet+}-AcH^{\bullet}$ at 298 K. (c) Time profiles of the absorption at 650 nm of $H_4DPOx^{\bullet+}-AcH^{\bullet}$ at 298 K. Inset: First-order plots.

−0.57 V in the presence of the bisporphyrin, due to the complex formation (see Supporting Information, S7). As a result, the free energy change of electron transfer to form the ET state is from 1.04 to 1.28 eV in the π-complex (Table 1). On the other hand, the E_{ox} value of H_2OEP (monomer porphyrin) exhibits a smaller potential shift in the presence of AcH^+ than in the case of the bisporphyrin (see Supporting Information, S8). This indicates that the large potential shift in $H_4DPOx-AcH^+$ mainly results from the insertion of AcH^+ between the two porphyrin rings of the bisporphyrin.

Photoinduced Electron Transfer in the $H_4DPOx-AcH^+$ Complex. The occurrence of photoinduced ET in the π-complex was confirmed by nanosecond laser flash photolysis. Figure 5 shows the transient absorption spectra of a PhCN solution containing both H_4DPOx and AcH^+ observed upon laser excitation. The strong absorption in the range from 450 to 540 nm is ascribed to $AcH^{\bullet}$,[25,39] although the absorption band due to $AcH^{\bullet}$ around 480 nm is overlapped by the absorption due to $H_4DPOx^{\bullet+}$. The transient absorption in the range from 620 to 800 nm is ascribed to $H_4DPOx^{\bullet+}$. The assignment of the transient species is confirmed by comparison with the absorption spectrum of $H_4DPOx^{\bullet+}$ in a PhCN solution containing AcH^+ (Figure 6a), which was obtained from the ET oxidation of the $H_4DPOx-AcH^+$ complex with $Ru(bpy)_3^{3+}$ (bpy = 2,2′-bipyridine). The absorption spectrum of $AcH^{\bullet}$ in PhCN solution was obtained from the photoinduced ET reduction of AcH^+ with ferrocene by photoexcitation of AcH^+ at 430 nm (Figure 6b).

The decay time profiles of the absorption at 520 nm with the different laser intensities are shown in Figure 7. The first-order plots afford good linear correlations with the same slope, irrespective of the different laser intensities. The decays at 460,

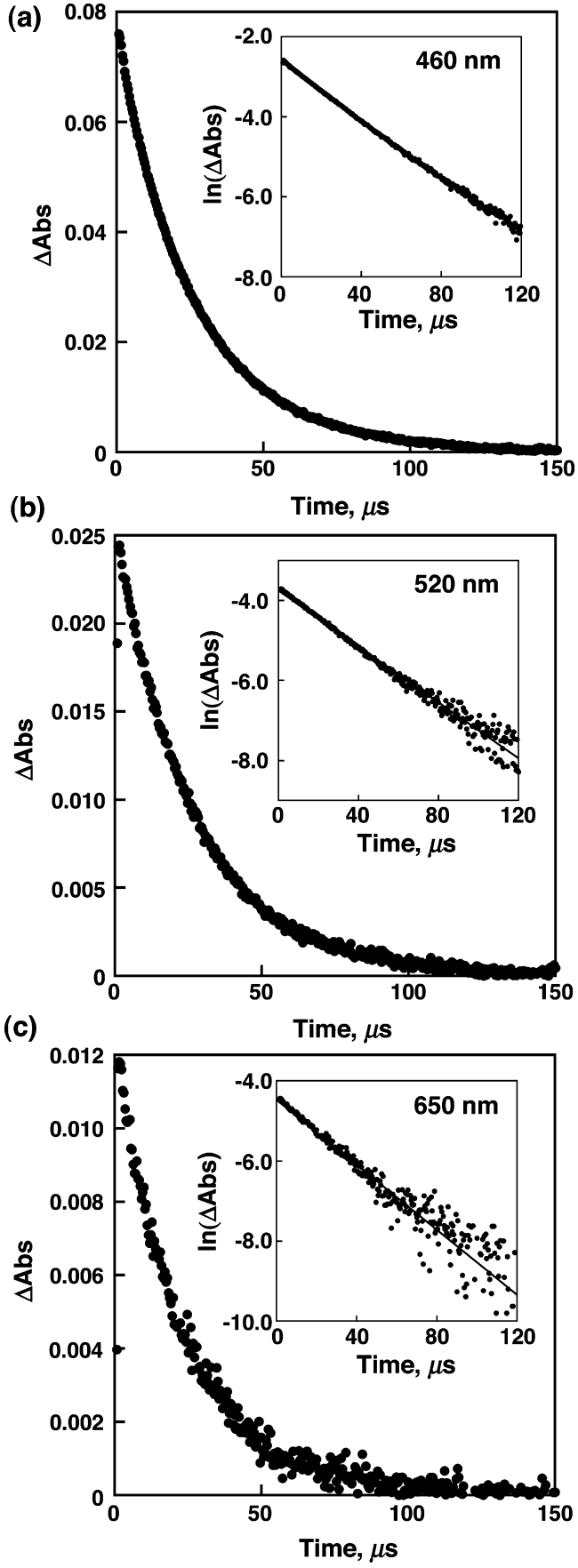

Figure 8. Time profiles of the absorption at (a) 460, (b) 520, and (c) 650 nm of $H_4DPOx^{\bullet+}-AcH^{\bullet}$ in deaerated PhCN. Insets: First-order plots.

(39) The absorption maximum of the acridinium ion is around 450−540 nm, which is confirmed by the photoinduced ET from ferrocene to AcH^+. The absorption spectrum of 9-phenyl-10-methylacridinyl radical has been reported. See: Ohkubo, K.; Suga, K.; Morikawa, K.; Fukuzumi, S. *J. Am. Chem.* Soc. **2003**, *125*, 12850, and ref 25a.

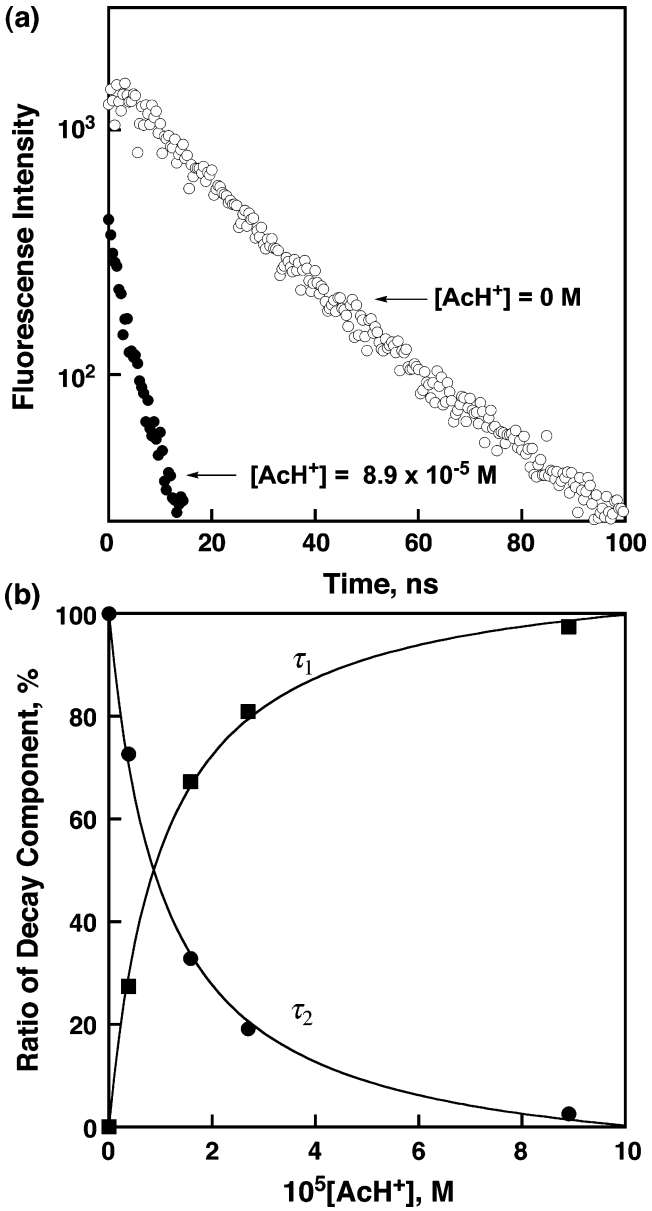

Figure 9. (a) Fluorescence decay profiles of $^1H_4DPOx^*$ at 631 nm in the absence and in the presence of AcH^+ in deaerated PhCN containing H_4-DPOx (1.0×10^{-5} M) at 298 K observed by excitation at 525 nm. (b) Ratio of the fast decay component (τ_1) and the slow decay component (τ_2) of $^1H_4DPOx^*$ vs concentration of AcH^+.

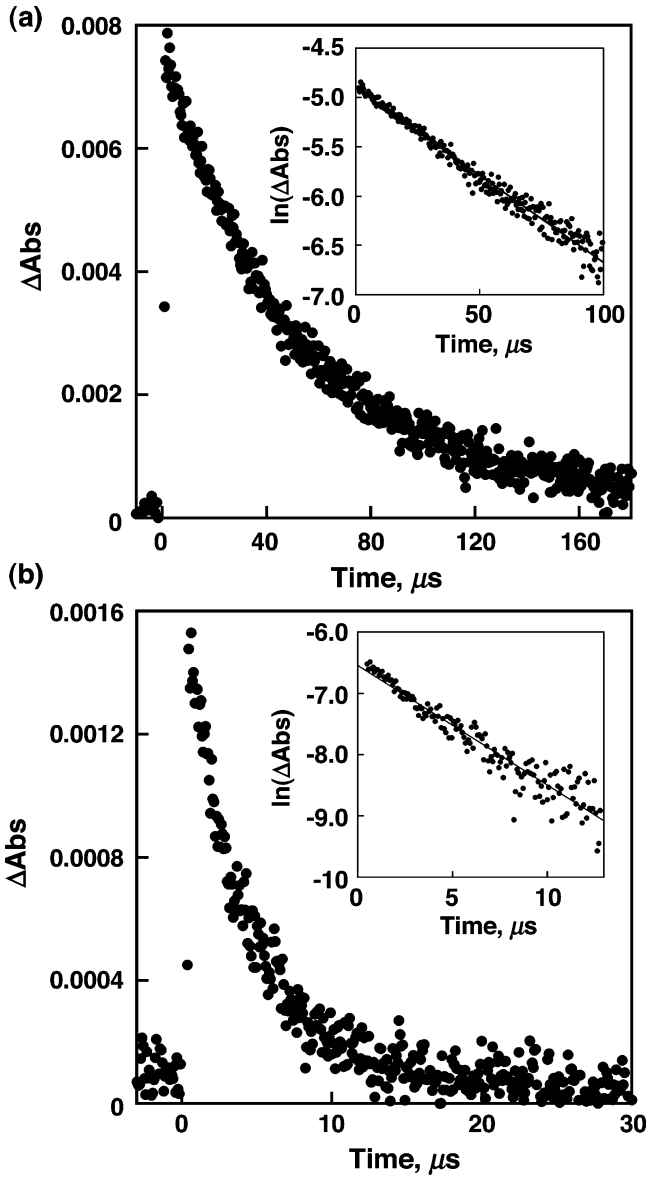

Figure 10. (a) Decay time profiles of the absorption at 520 nm of H_4-$DPOx^{\bullet+}$−$AcH^\bullet$ in deaerated PhCN, obtained upon nanosecond flash photolysis at 273 K. (b) Decay time profiles at 353 K.

520, and 650 nm obey first-order kinetics with the same slope (Figure 8a−c). Such a first-order decay with the same slope strongly indicates that the back electron transfer (BET) from $AcH^\bullet$ to $H_4DPOx^{\bullet+}$ occurs in the π-complex and that no bimolecular decay is involved. The lifetime of the ET state is determined as 18 μs at 298 K ($k_{BET} = 5.5 \times 10^4$ s^{-1}). There was no spectral change after the laser flash photolysis measurements. This indicates that no net chemical reaction has occurred other than the photoinduced ET followed by the BET to the ground state.[40] The quantum yield of the ET state at 298 K is determined as 0.90 ± 0.05 from the absorption of $H_4DPOx^{\bullet+}$−$AcH^\bullet$ ($\epsilon_{680} = 3900$ M^{-1} cm^{-1}),[41] using the absorbance of the triplet−triplet absorption of H_2TPP (TPP = tetraphenylporphyrin, $\epsilon_{690} = 3500$ M^{-1} cm^{-1})[42] as a reference.

The rate constant (k_{ET}) of ET from the singlet excited state of H_4DPOx ($^1H_4DPOx^*$) to AcH^+ in the H_4DPOx−AcH complex was determined by measuring the time-resolved fluorescence. Figure 9a shows the time-resolved fluorescence decays of a PhCN solution containing H_4DPOx in the absence and in the presence of AcH^+, observed by excitation at 631 nm. The emission decay of H_4DPOx in the presence of AcH^+ (8.9×10^{-5} M) becomes faster than the decay in the absence of AcH^+ due to ET from $^1H_4DPOx^*$ to AcH^+. The k_{ET} value is determined from the faster component (τ_1) of the fluorescence lifetime as 2.9×10^8 s^{-1}. The ratio of the faster component (τ_1) increases with increasing concentration of AcH^+ to reach 100%, whereas the slow component (τ_2) decreases to zero (Figure 9b). This also results from the π-complex formation as

(40) Such an ET state could not be observed by photoirradiation of a PhCN solution containing H_2OEP and AcH^+, probably due to the larger λ value of BET. Upon photoexcitation, there is no ET state observed.

(41) The ϵ value of $H_4DPOx^{\bullet+}$ has been determined by ET oxidation of the H_4DPOx−AcH^+ complex with $Ru(bpy)_3^{3+}$.

(42) (a) Pekkarinen, L.; Linschitz, H. *J. Am. Chem. Soc.* **1960**, *82*, 2407. (b) Gratz, H.; Penzkofer, A. *Chem. Phys.* **2000**, *254*, 363.

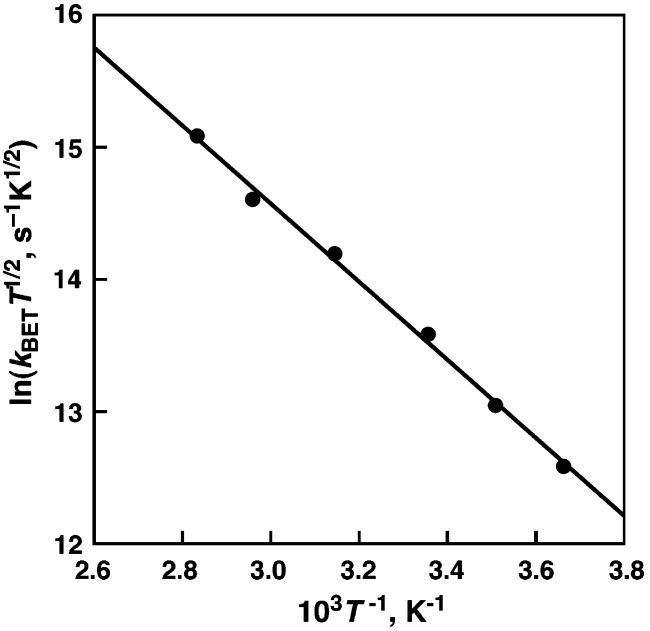

Figure 11. Plot of $\ln(k_{BET}T^{1/2})$ versus T^{-1} for the intramolecular BET in $H_4DPOx^{\bullet+}-AcH^{\bullet}$ in PhCN determined by laser flash photolysis.

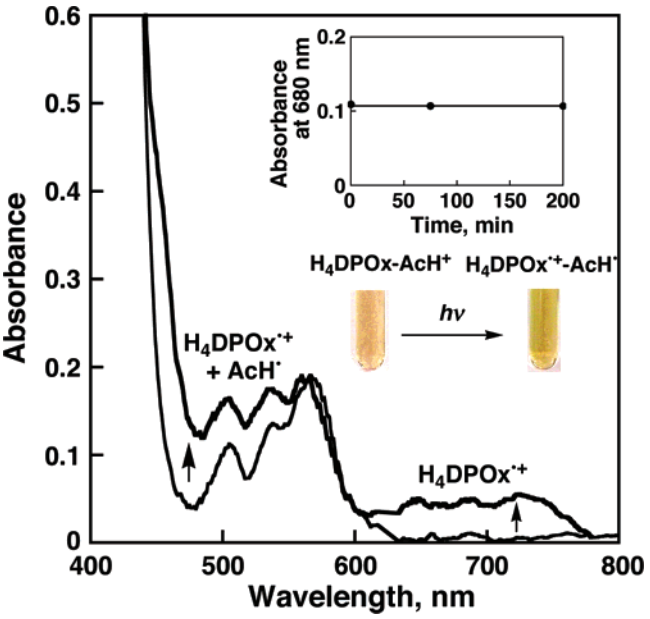

Figure 12. Visible absorption spectra obtained by photoirradiation with a high-pressure mercury lamp of deaerated 2-MeTHF/butyronitrile (9:1 v/v) glasses of H_4DPOx (1.8×10^{-5} M) and AcH^+ (3.6×10^{-4} M) at low temperature and measured in liquid N_2 dewar at 77 K. Inset: Time profile at 680 nm and images before and after photoirradiation at low temperatures, measured at 77 K.

AcH^+ is inserted between the two porphyrin rings of H_4DPOx. The binding constant can also be determined from the saturated dependence of Figure 9b as 96 000 ± 7000 M^{-1}. This value agrees with that obtained from the UV−visible absorption change (97 000 ± 1000 M^{-1}) in Figure 1.

The energy diagram of the $H_4DPOx-AcH^+$ complex is summarized in Scheme 2. The energy level of the singlet excited state of H_4DPOx is 1.97 eV, which is determined from the absorption and fluorescence spectra.[43] The energy level of the triplet excited state of H_4DPOx is 1.59 eV, which is determined from the phosphorescence spectrum observed in deaerated frozen 50% EPA and 50% ethyl iodide at 77 K (see Supporting Information, S9).[44] The energy level of the ET state ($-\Delta G_{ET}$) in the π-complex is determined as 1.28 eV from the redox potentials of the π-complex (Table 1). It is important to note that the energy level of the ET state of the $H_4DPOx-AcH^+$ complex is lower than those of the triplet states of H_4DPOx (1.59 eV) and AcH^+ (2.01 eV).[45,46] This is the reason why the transient absorption spectra due to the ET state can be observed instead of the T−T absorption spectrum.

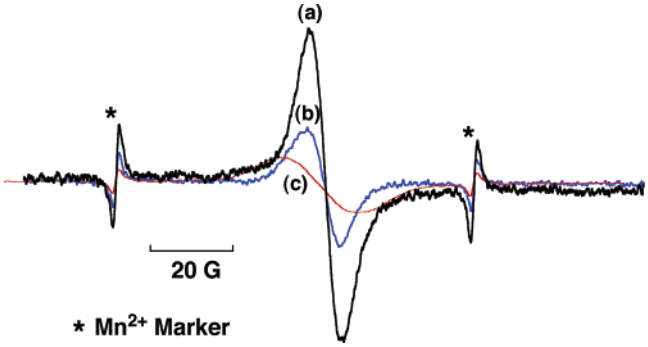

Figure 13. (a) ESR spectrum of a deaerated PhCN solution of H_4DPOx (3.2×10^{-5} M) and AcH^+ (1.6×10^{-4} M) photoirradiated with a high-pressure mercury lamp at low temperature and measured at 173 K. (b) ESR spectrum of a deaerated PhCN/CH_3CN (9:1 v/v) solution of H_4DPOx (1.0×10^{-4} M) and $Ru(bpy)_3^{3+}$ (1.0×10^{-4} M) observed at 173 K. (c) ESR spectrum of a deaerated PhCN solution of AcH^+ (1.1×10^{-2} M) and Fc (1.7×10^{-2} M) photoirradiated with a high-pressure mercury lamp at low temperature and measured at 173 K.

The ET state lifetimes in PhCN have also been determined in the range from 273 to 353 K by laser flash photolysis (Figure 10). The lifetime of the ET state exhibits a large temperature dependence. The temperature dependence of the rate constant of back electron transfer (k_{ET}) is in accordance with the Marcus equation (eq 2),[47] where V is the electronic coupling matrix

$$\ln(k_{ET}T^{1/2}) = \ln\left(\frac{2\pi^{3/2}V^2}{h(\lambda k_B)^{1/2}}\right) - \frac{(\Delta G_{ET} + \lambda)^2}{4\lambda k_B T} \qquad (2)$$

element, h is the Planck constant, k_B is the Boltzmann constant, T is the absolute temperature, and ΔG_{ET} is the free energy change of back electron transfer to the ground state. The plot of $\ln(k_{ET}T^{1/2})$ vs T^{-1} (eq 2) is linear, as shown in Figure 11, and from the slope and the intercept, the λ and V values are determined as 0.54 ± 0.1 eV and 1.6 ± 0.3 cm^{-1}, respectively.[48]

The ET state lifetime at 77 K, extrapolated from the linear plot in Figure 11, is obtained as 360 days. Such an extremely long-lived ET state is indeed detected by the steady-state

(43) The energy of the 0−0 transition between the S_1 and the S_0 states was determined by averaging the energies of the corresponding (0,0) peaks in the fluorescence and the absorption bands. See: (a) Luo, C.; Guldi, D. M.; Imahori, H.; Tamaki, K.; Sakata, Y. *J. Am. Chem. Soc.* **2000**, *122*, 6535. (b) Imahori, H.; Yamada, K.; Yoshizawa, E.; Hagiwara, K.; Okada, T.; Sakata, Y. *J. Porphyrins Phthalocyanines* **1997**, *1*, 55.

(44) (a) Gouterman, M.; Khalil, G. E. *J. Mol. Spectrosc.* **1974**, *53*, 88. (b) Darwent, J. R.; Douglas, P.; Harriman, A.; Porter. G.; Richoux, M.-C. *Coord. Chem. Rev.* **1982**, *44*, 83.

(45) Kikuchi, K.; Sato, C.; Watabe, M.; Ikeda, H.; Takasaki, Y.; Miyashi, T. *J. Am. Chem. Soc.* **1993**, *115*, 5180.

(46) Fukuzumi, S.; Ohkubo, K.; Imahori, H.; Shao, J.; Ou, Z.; Zheng, G.; Chen, Y.; Pandey, R. K.; Fujitsuka, M.; Ito, O.; Kadish, K. M. *J. Am. Chem. Soc.* **2001**, *123*, 10676.

(47) (a) Marcus, R. A. *Angew. Chem., Int. Ed. Engl.* **1993**, *32*, 1111. (b) Marcus, R. A.; Sutin, N. *Biochim. Biophys. Acta* **1985**, *811*, 265.

(48) For other examples of large temperature dependence of k_{BET}, see: Ohkubo, K.; Kotani, H.; Shao, J.; Ou, Z.; Kadish, K. M.; Li, G.; Pandey, R. K.; Fujitsuka, M.; Ito, O.; Imahori, H.; Fukuzumi, S. *Angew. Chem., Int. Ed.* **2004**, *43*, 853, and ref 26.

Scheme 2

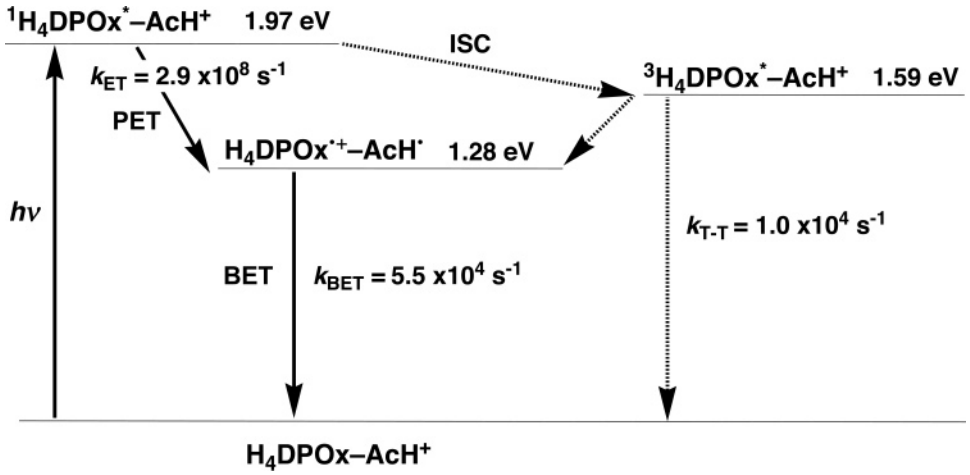

photoirradiation of glassy 2-MeTHF containing a 10% butyronitrile solution of $H_4DPOx-AcH^+$ by a 1000 W high-pressure mercury lamp at low temperature. The new absorption bands due to $H_4DPOx^{\bullet+}$ (450−540 and 620−800 nm) and $AcH^\bullet$ (450−540 nm) are clearly observed, as shown in Figure 12. The observed ET state exhibits no decay for 200 min at 77 K (inset of Figure 12). The color change on going from the ground state of the $H_4DPOx-AcH^+$ complex to the ET state is also shown in the inset of Figure 12. It is important to note that the color and the absorption spectrum of the ET state go back to the original ones when the temperature is increased to 298 K, and such a change can be repeated many times. The large temperature dependence of the rate constant of BET (Figure 12) results from the small λ value (0.54 ± 0.01 eV) in the π-complex when the BET is deeply in the Marcus inverted region.

Since the λ and V values are determined from the temperature dependence of k_{BET}, the driving force dependence of the ET rate constant in the π-complex at 298 K is obtained according to eq 2 (see Supporting Information, S10). The k_{ET} value of electron transfer from $^1H_4DPOx^*$ to AcH^+ in the $H_4DPOx-AcH$ complex (vide supra) agrees with the value predicted from the Marcus curve within experimental error (open circle in S10). The forward ET is nearly on the Marcus top region, whereas the BET process is deeply in the Marcus inverted region. This is the reason why an extremely long-lived ET state of the π-complex is formed in PhCN.

The formation of the ET state was further confirmed by ESR measurements under photoirradiation of the π-complex in frozen PhCN at 173 K. The observed ESR signal ($g = 2.0034$) is shown in Figure 13 (part a), where the ESR signal of $H_4DPOx^{\bullet+}$ ($g = 2.0031$) obtained from the ET oxidation of H_4DPOx with $Ru(bpy)_3^{3+}$ (part b) and that of $AcH^\bullet$ ($g = 2.0036$) obtained from the photoinduced ET reduction of AcH^+ with ferrocene (part c) are also shown for comparison. The observed ESR signal (Figure 13a) is composed of the superposition of the ESR signals of $H_4DPOx^{\bullet+}$ (Figure 13b) and $AcH^\bullet$ (Figure 13c) and thus is assigned to the ET state ($H_4DPOx^{\bullet+}-AcH^\bullet$).

In conclusion, a 1:1 π-complex is formed between H_4DPOx and AcH^+ in PhCN with a large binding constant. The redox potentials of H_4DPOx and AcH^+ are changed due to the π-complex formation. The surprisingly persistent ET state of the π-complex has been attained upon photoexcitation of the π-complex at low temperature. The small reorganization energy of electron transfer has made it possible to attain fast photoinduced electron transfer but extremely slow back electron transfer in the π-complex.

Acknowledgment. This work was partially supported by a Grant-in-Aid (No. 17550058) from the Ministry of Education, Culture, Sports, Science and Technology, Japan. Financial support from the CNRS (UMR 5633) is also acknowledged.

Supporting Information Available: Procedure for the synthesis of H_4DPOx, full list of authors of ref 35, Job's plot for complexation of H_4DPOx with AcH^+, ^1H NMR spectral change in the formation of H_2OEP with AcH^+, CV and SHACV of AcH^+ with H_4DPOx, DPV of H_2OEP with AcH^+, phosphorescence spectrum of H_4DPOx at 77 K, and Marcus driving force dependence of intramolecular ET rate constants. This material is available free of charge via the Internet at http://pubs.acs.org.

JA064678B